Photodissociation Dynamics of BH_3CO at 193 nm

Brad R. Weiner,*,† L. Pasternack, H. H. Nelson,

Chemistry Division, Code 6111, Naval Research Laboratory, Washington, D.C. 20375-5000

K. A. Prather, and R. N. Rosenfeld

Department of Chemistry, University of California, Davis, California 95616 *(Received: September 28, 1989; In Final Form: December 7, 1989)*

The photodissociation dynamics of the reaction $BH_3CO \rightarrow BH_3 + CO$ at 193 nm have been investigated by using time-resolved infrared absorption spectroscopy and ultraviolet/visible emission spectroscopy. Partitioning of the available energy into the translational and vibrational degrees of freedom has been measured for the nascent CO photofragment. Time-resolved carbon monoxide laser absorption spectroscopy has been used to observe the CO photofragment in vibrationals levels $v'' = 0$–4. The nascent CO photofragment can be characterized by a vibrational temperature, $T_{vib} = 2760 \pm 160$ K. A lower limit to the CO translational energy, $E_{trans}(v''=0) \geq 5$ kcal/mol, has been established by measuring the Doppler profile of two CO absorption lines with a tunable diode laser absorption system. Time-resolved tunable diode laser absorption spectroscopy has also been employed to observe internal excitation in the nascent BH_3 photofragment, as well as measure the quantum yield for its production from BH_3CO photolysis. A lower limit for the quantum yield, $\Phi_{193}(BH_3) \geq 0.7^{+0.3}_{-0.2}$, has been established. By comparison with limiting case models, we conclude that the photodissociation of BH_3CO at 193 nm leads to a nonstatistical partitioning of energy into the BH_3 fragment.

Introduction

Time-resolved descriptions of the photodissociation of small (tri- and tetraatomic) molecules have been the target of many laboratories in recent years. For the most part, comprehensive measurements of the energy partitioning into the photoproducts[1] and the vector correlations between photofragment velocity and rotational angular momentum[2] have been the primary methods used to understand the detailed reaction dynamics. Most recently, experiments on the femtosecond time scale spectroscopically capture the actual bond fission in small polyatomic molecules.[3] Understanding the photodissociation dynamics of larger molecules ($\geq$5 atoms) in this detail, however, remains a complex problem. Additional degrees of freedom open up new pathways for the deposition of available energy, and multiple product channels require a complete characterization of the photoinitiated chemistry. Quantitative energy disposal data on more than one degree of freedom and branching ratio measurements in polyatomic photodissociation reactions remain essential to unraveling the dynamics. This can be especially true for weakly bound molecules, where there is a large amount of energy available to be partitioned among the photofragments, and where secondary "thermal" (statistical) fragmentations are feasible.

Borane carbonyl (BH_3CO) is a very attractive molecule for the polyatomic photodissociation dynamics studies described above, since both of the primary photoproducts, BH_3 and CO, as well as the other possible boron hydride products can be probed spectroscopically. BH_3CO has been photolyzed with an ArF excimer laser at 193 nm to yield the products BH_3[4,5] and BH[6] and with a conventional flashlamp to yield BH[7,8] and BH_2.[9] Little is known about the photoproduction dynamics of these species.

An energy level diagram for the energetically allowed channels in the BH_3CO ultraviolet photodissociation system is shown in Figure 1. Formation of the products BH_3 and CO requires only 20.6 kcal/mol,[10] which leaves 127 kcal/mol available for distribution into the product degrees of freedom (E_{avl} in Figure 1). BH_3CO is known to have a structure consisting of a pyramidal BH_3 unit (compared to the planar geometry of free BH_3), and a CO bond length very nearly that of free CO (1.135 vs. 1.128 Å).[11] For an impulsive dissociation, one might expect a large amount of internal energy in the BH_3 photofragment, primarily in the umbrella bending mode (ν_2). In fact, there may be enough energy in the nascent BH_3 for it to decompose unimolecularly into the secondary products BH and H_2 (or BH_2 + H), which would explain the observation of BH (BH_2) in this system.

Recently, Pasternack et al. have reported the rotational energy distribution of the CO fragment in the 193-nm photodecarbonylation of borane carbonyl.[12] They found that the nascent CO is rotationally "cold" with the photofragments, formed in $v'' = 0$ and $v'' = 1$, characterized by rotational temperatures of 362 and 175 K, respectively. In this paper, we report information about the kinetic and internal energy distributions of the BH_3 and CO products following 193-nm photolysis of BH_3CO, as well as a quantum yield for the production of BH_3 as a final stable product. Internal excitation in BH_3 has been observed by using tunable diode laser absorption spectroscopy (TDLAS). Although we cannot quantitatively measure the amount of internal energy in the BH_3 fragment because only the ground electronic and vibrational levels have been spectroscopically identified, we observe a rise time for the appearance of the ground vibrational state of the BH_3 fragment, suggesting that the nascent BH_3 has significant internal energy. A nascent vibrational energy distribution ($v'' = 0$–4) of the CO photofragment is observed by using time-resolved carbon monoxide laser absorption spectroscopy following the 193-nm photodissociation of BH_3CO. We have also

* To whom correspondence should be sent.

† NRC/NRL Postdoctoral Research Associate (1986–1988). Current address: Department of Chemistry, University of Puerto Rico, Rio Piedras, Puerto Rico 00931.

(1) Ashfold, M. N. R., Baggot, J. E., Eds. *Advances in Gas-Phase Photochemistry and Kinetics: Molecular Photodissociation Dynamics*; The Royal Society of Chemistry: London, 1987.

(2) (a) Dixon, R. N. *J. Chem. Phys.* **1986**, *85*, 1866. (b) Houston, P. L. *J. Phys. Chem.* **1987**, *91*, 5388.

(3) Rosker, M. J.; Dantus, M.; Zewail, A. H. *J. Chem. Phys.* **1988**, *89*, 6113, 6128.

(4) Kawaguchi, K.; Butler, J. E.; Yamada, C.; Bauer, S. H.; Minowas, T.; Kanamori, H.; Hirota, E. *J. Chem. Phys.* **1987**, *87*, 2438.

(5) Pasternack, L.; Balla, R. J.; Nelson, H. H. *J. Phys. Chem.* **1988**, *92*, 1200.

(6) Rice, J. K.; Caldwell, N. J.; Nelson, H. H. *J. Phys. Chem.* **1989**, *93*, 3900.

(7) Bauer, S. H.; Herzberg, G.; Johns, J. W. C. *J. Mol. Spectrosc.* **1964**, *13*, 256.

(8) Johns, J. W. C.; Grimm, F. A.; Porter, R. F. *J. Mol. Spectrosc.* **1967**, *22*, 435.

(9) Herzberg, G.; Johns, J. W. C. *Proc. R. Soc. London* **1966**, *298a*, 142.

(10) Bauer, S. H. In *Advances in Boron and the Boranes*; Liebman, J. F., Greenberg, A., Williams, R. E., Eds.; VCH Publishers: New York, 1988; pp 391–415.

(11) Venkatachar, A. C.; Taylor, R. C.; Kuczkowski, R. L. *J. Mol. Struct.* **1977**, *38*, 17.

(12) Pasternack, L.; Weiner, B. R.; Baronavski, A. P. *Chem. Phys. Lett.* **1989**, *154*, 121.

0022-3654/90/2094-4138$02.50/0

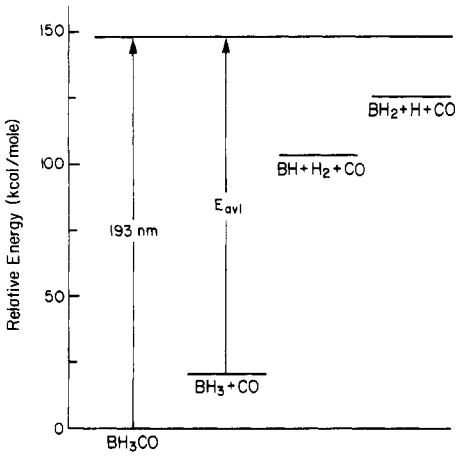

Figure 1. Thermochemically allowed processes in the photolysis of BH_3CO at 193 nm. E_{avl} represents the amount of energy available to be partitioned to the BH_3 and CO photoproducts.

determined a lower limit to the nascent CO photofragment translational energy by measuring the Doppler profile of two CO absorption lines with TDLAS.

Experimental Section

Tunable Diode Laser Absorption Spectroscopy Measurements. The apparatus used in these experiments has been described in detail previously.[5] Briefly, the reaction cell consists of a 2-m Pyrex tube (4-cm diameter) fitted with BaF_2 windows. BH_3CO is photolyzed by using an ArF (193 nm) excimer laser (Lambda Physik, Model 201 MSC) at a fluence of 5–50 mJ/cm^2. The photolysis products are probed in absorption with a tunable diode laser (Laser Analytics, Model LS-3). The pump and probe beams are collinear over the 2-m cell length. After a single pass through the reaction cell, the infrared radiation from the diode laser is dispersed by a 0.5-m monochromator, which selects a single laser emission mode, and is detected by a HgCdTe detector (risetime $\approx$ 1 μs).

Both BH_3 and CO can be detected by this infrared absorption technique. The BH_3 is measured near 1141 cm^{-1}, the frequency of the ν_2 umbrella vibration. NH_3 is used for wavelength calibration in this region. The CO is measured in the wavelength region 2100–2170 cm^{-1}, which encompasses some of the P and R lines for CO ($v'' = 0$–4). Wavelength calibration is performed by comparison to N_2O (300 K) or CO (300 K), or in the case of CO ($v'' > 0$) a 1-m electric discharge tube with a mixture of CO in helium was used. The frequency of the diode laser can be locked to the frequency of a selected CO line in the discharge by using a PAR Model 124A lock-in amplifier.

Product appearance and yield measurements are made by tuning the diode laser to the frequency of the absorption feature of interest and directing the output of the detector to a digital oscilloscope (LeCroy Model 9400) which is triggered in sync with the photolysis laser. The oscilloscope digitizes and averages the transient waveform over 50–500 experimental repetitions. The averaged waveform is then transferred to a microcomputer (IBM PC-AT) for analysis and storage. For the measurement of the Doppler profile of an absorption feature, the diode laser frequency is swept across the absorption by stepping the diode current. The frequency response of the laser diode to changes in the current is measured by using a solid Ge etalon with a 0.047-cm^{-1} free spectral range. The transient absorption signals are sampled with a gated integrator (Stanford Research Systems Model SR250) and digitized and stored by the microcomputer. Typically, the signal from 20 laser shots is averaged at each current step.

Electronic Emission Measurements. Prompt product emission (visible and ultraviolet) following 193-nm photolysis is monitored by using a small (ca. 100 cm^3) fluorescence cell mounted directly in front of the entrance slit of a 0.5-m monochromator (Acton Model VM505). The monochromator is scanned from 300 to 900 nm. Product emission is detected by a photomultiplier tube (RCA Model 31034A), and the signal is sampled by the gated integrator and processed by the microcomputer.

Time-Resolved CO Laser Absorption Measurements. The experimental apparatus has been described in detail previously.[13] The CO precursor, BH_3CO (0.002–0.050 Torr), is diluted in buffer gas (He, Ar, or SF_6) in a 1-m Pyrex absorption cell fitted with CaF_2 windows. Pressures are measured with a capacitance manometer (MKS Instruments, Baratron 220B). The absorption cell is irradiated with the 193-nm output of an ArF excimer laser (Lambda Physik, Model EMG-101, 15-ns pulse width) at a fluence of 1–10 mJ/cm^2. A continuous-wave, grating tuned, carbon monoxide laser propagates through the absorption cell coaxially with the excimer laser. The two laser beams were made coincident with a dichroic mirror (Acton Research Corp.), and a second dichroic was used to prevent the 193-nm radiation from hitting the infrared detector. The infrared intensity is monitored with a 77 K InSb detector (time constant $\approx$ 100 ns). The CO laser signal is amplified and digitized by a LeCroy 8837 transient digitizer, and sent to a microcomputer for signal averaging and data analysis. Typically, 30–200 transients are averaged in a single experiment.

In all the experiments, BH_3CO was prepared by heating a high-pressure (10–12 atm) mixture of B_2H_6 and CO, following the method described by Bethke and Wilson.[14] The crude product was purified by trap-to-trap distillation prior to use. The sample could be stored for long periods (months) at 77 K, without significant decomposition.

Results

Energy Distribution in the BH_3 Product. We have measured the time-resolved absorption of the ground vibrational and electronic state of BH_3 (ν_2, $v'' = 0$, $J'' = 6$), following 193-nm photolysis of BH_3CO by using tunable diode laser absorption spectroscopy at 1141.025 cm^{-1}. No measureable nascent ground-state population of BH_3 is observed at 0.9 Torr of total pressure with 5 mTorr of BH_3CO and N_2 buffer gas. Under these conditions, the ground-state BH_3 concentration increases in time, from an unmeasurably small level, for 60 μs after the BH_3CO photolysis. The BH_3 rise time decreases to <3 μs at 7.6 Torr of total pressure. The decrease in the rise time supports the assumption that a significant fraction of the excess energy from the photolysis is partitioned into internal degrees of freedom in the BH_3 photofragment. The variation of the rise time with added quencher gas is consistent with vibrational quenching, assuming a V→T,R rate of $\sim 10^{-12}$ cm^3 s^{-1} molecule^{-1}.[15] The infrared spectroscopy of higher vibrational levels of BH_3 is unknown, so we are unable to quantitatively determine the amount of vibrational excitation in the BH_3 fragment. Control experiments with B_2H_6 as an alternative borane source confirmed that we were indeed looking at BH_3 (ν_2, $v'' = 0$).

An emission spectrum following the photolysis of BH_3CO was recorded in an attempt to observe electronic excitation in the BH_3 fragment. We were unable to detect any emission due to single photon 193-nm absorption (fluence $\lesssim$50 mJ/cm^2). At higher photolysis fluence levels, we observe emission from B, BH, and possibly BH_2 formed in multiphoton processes. The electronic spectra of BH_3 has not been unambiguously assigned. The lowest excited singlet and triplet states of BH_3 have been calculated to lie 6.08 and 5.48 eV, respectively, above the ground state.[16] These energies are inaccessible in this experiment for single-photon 193-nm absorption.

Vibrational Distribution of the CO Product. Nascent CO, resulting from the photolysis of BH_3CO, was observed in vibrational levels $v'' = 0$–4 by using time-resolved CO laser absorption. In these experiments, time-resolved absorption of a CO rovibrational line ($P_{v+1,v}(J)$ CO laser transitions where $J = 11$, 10, 9, and

(13) Sonobe, B. I.; Fletcher, T. R.; Rosenfeld, R. N. *Chem. Phys. Lett.* **1984**, *105*, 322.
(14) Bethke, G. M.; Wilson, M. K. *J. Chem. Phys.* **1957**, *26*, 1118.
(15) Baughcum, S. L.; Leone, S. R. *J. Chem. Phys.* **1980**, *72*, 6531.
(16) Swope, W. C.; Schaefer III, H. F.; Yarkony, D. R. *J. Chem. Phys.* **1980**, *73*, 407.

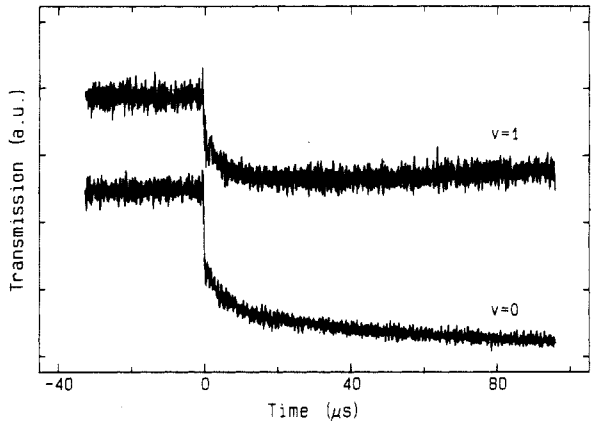

Figure 2. Time-resolved absorption of the $P_{2,1}(11)$ and $P_{1,0}(10)$ CO laser lines following photodissociation of BH_3CO at 193 nm. The UV laser fluence was 8.0 mJ/cm^2, [BH_3CO] = 0.025 Torr, and [He] = 5.0 Torr.

8 for $v'' = 0$–4, respectively) was monitored following 193-nm photolysis of BH_3CO. Representative transient absorption curves are shown in Figure 2. Data corresponding to low vibrational levels, CO ($v'' = 0$–2), show a fast rise time (detector limited) followed by a slower rise and decay of the CO absorption. For CO ($v'' = 4$), only a single fast rise is observed. No signal was observed for CO ($v'' > 4$). Helium, at 5 Torr, was used as a buffer gas, which was sufficient for rotational thermalization but not vibrational relaxation of the CO photofragment. A linear dependence of CO population on photolysis laser fluence was observed over the range 2.5–9.5 mJ/cm^2, suggesting that the CO is produced by a one-photon-absorption process.

The relative vibrational populations were determined from the amplitude of the prompt transient absorption signal (measured 500 ns following photolysis) for each $P_{v+1,v}(J)$ CO laser line up to the highest vibrational level where absorption could be detected, in this case CO ($v'' = 4$). The relative vibrational level populations are obtained by[17]

$$N_v \sim \sum_{i=v}^{v_m} \left(\frac{2J+1}{2J-1}\right)^{i} \left(\frac{H_{i+1}}{i+1}\right) \qquad (1)$$

where v_m is the maximum observed CO vibrational level and H_{v+1} is the absorption intensity of the $P_{v+1,v}(J)$ CO laser line. This expression assumes the harmonic oscillator approximation, which, in this case, introduces a very small (≤2.5%) error. The relative nascent vibrational populations, N_0:N_1:N_2:N_3:N_4 are 1.00 (±0.02):0.33 (±0.02):0.11 (±0.03):0.03 (±0.03):0.0012 (±0.03). These results are displayed in Figure 3. The solid line represents the best straight-line Boltzmann fit to the data and corresponds to a vibrational temperature of 2760 ± 160 K. The average vibrational energy of the CO formed in the dissociation is 5.9 kcal/mol. Experiments performed at BH_3CO pressures of 10 and 25 mTorr gave the same results within experimental error. This result indicates that the CO vibrational energy distribution results from the primary photochemistry of BH_3CO.

CO Translational Energy. We measure the translational energy of a state-specific CO fragment by measuring the line profile of a CO ($v'' = 0$) absorption line. The total pressure is maintained as low as possible, and the measurements are taken as close as possible in time to the photolysis laser pulse to reduce collisions. We estimate that under our experimental conditions ([BH_3CO] = 6 mTorr, [N_2] = 0 and 2 μs delay), an average of 0.4 collisions take place prior to measurement of the line profile. The results of a measurement of the $P_{1,0}(8)$ CO line are shown in Figure 4a. This spectrum represents the sum of three scans, each of which averages 20 laser shots per step. The line profile of the $P_{1,0}(14)$ line is the same within experimental error. For comparison, we also show (cf. Figure 4b) the Doppler profile of a collisionally relaxed CO photofragment ([BH_3CO] = 8 mTorr, [N_2] = 1.0 Torr) obtained 50 μs after the excimer laser pulse. The solid line is a simulation of a Doppler-broadened CO absorption line ($\Delta\nu_D$ = 0.0049 cm^{-1}) at 300 K.

(17) Houston, P. L.; Moore, C. B. *J. Chem. Phys.* **1976**, *65*, 757.

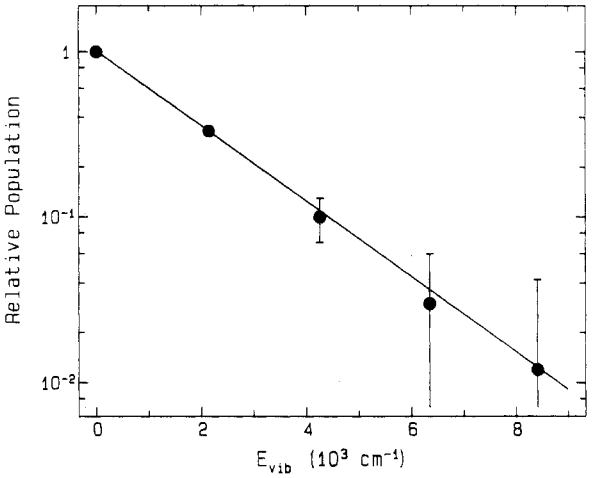

Figure 3. Relative vibrational populations of the nascent CO resulting from the photodissociation of BH_3CO at 193 nm. The signal intensities were measured 500 ns after the excimer laser fired, and the populations were determined from eq 1. The straight line is obtained from a linear least-squares fit to the data and corresponds to a vibrational temperature of 2760 ± 160 K.

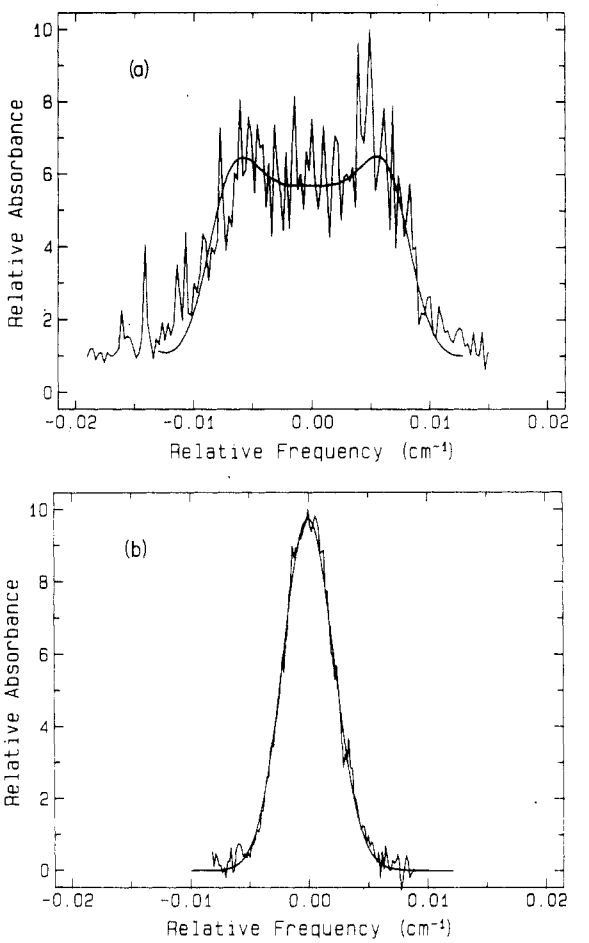

Figure 4. Absorption line shapes observed for the $P_{1,0}(8)$ transition of CO following photodissociation of BH_3CO at 193 nm. These Doppler profiles are measured at the following delays (time after excimer laser fires) and pressures: (a) Delay = 2 μs, [BH_3CO] = 0.006 Torr, no buffer gas; the solid line represents calculated line shapes, obtained by using a rectangular distribution convoluted with a Gaussian function for both the upper and lower states. (b) Delay = 50 μs, [BH_3CO] = 0.008 Torr, [N_2] = 1.0 Torr; the solid line represents a simulation of a Doppler-broadened CO absorption ($\Delta\nu_D$ = 0.0049 cm^{-1}) at 300 K. See text for further explanation.

The analysis of the line shape in Figure 4a is complicated by a number of factors, including the initial BH_3CO thermal energy, the excimer laser frequency distribution, and the BH_3 rovibrational energy. Since CO is formed in several vibrational levels, the observed spectral line shape will take a form proportional to the difference in populations of the upper and lower states. If we ignore the spreads in parent initial energy, the BH_3 internal energy distribution, and the excimer laser width, the CO photofragment translational energy should have a single value corresponding to each of its rovibrational levels. If we assume that the fragment CO is ejected isotropically from the BH_3CO, the velocity distribution will be in the form of the surface of a sphere in the center-of-mass coordinate system. This distribution is observed as a Doppler shift when using an absorption technique as a probe. The width of the frequency distribution corresponds to the maximum Doppler shift determined by the available energy, and the area of the peak is proportional to the population in the rovibrational level. The shape of the absorption profile in this limiting case is calculated to be rectangular. Because the upper state of the CO rovibrational transition ($v'' = 1, J'' = 7$) is expected to have less translational energy than the lower state ($v'' = 0, J'' = 8$), the observed line shape, which is proportional to the difference in populations of the two states, will be double peaked. This is similar to the line shape observed by Kanamori and Hirota[18] in CS_2 photodissociation.

As described earlier, the line shape is broadened by the spreads in the initial BH_3CO thermal energy, the excimer laser photon energy, and the BH_3 internal energy distribution. Although the first two effects are small, we have observed significant excitation in the BH_3 photofragment. We include this spread in energy by convoluting the rectangular line profile discussed above with a Gaussian distribution. The relative areas of the frequency distributions of the upper and lower state are determined by the relative population of the CO ($v'' = 0$) and CO ($v'' = 1$) levels, which we have measured to be 1.00:0.33. With this model for the line shape, we obtain the best fit to the data with CO photofragment kinetic energies, E_{trans}, of E_{trans} ($v'' = 0$) = 5 ± 1 kcal/mol (center with a hwhm = 2 kcal/mol) and E_{trans} ($v'' = 1$) = 3 ± 1 kcal/mol center with a hwhm = 2 kcal/mol). This corresponds to rectangular and Gaussian line profiles of 0.006 cm^{-1} hwhm and 0.003 cm^{-1} hwhm, respectively. This fit is shown as the solid line in Figure 4b. Consequently, the total translational energy for the BH_3 and CO photofragments is ≥15 kcal/mol. This is a lower limit to the total translational energy due to collisional cooling. At shorter delay times, the absorption width is broadened to the extent that our signal-to-noise ratio is too low to reliably measure the line profile.

Quantum Yield for BH_3 Production. We have measured the quantum yield, $\Phi_{193}(BH_3)$, of BH_3 from 193-nm photolysis of BH_3CO to be $>0.7^{+0.3}_{-0.2}$. This was determined by measuring the infrared absorption due to BH_3 produced by the 193-nm photodissociation of BH_3CO compared to that from B_2H_6 with the tunable diode laser system. In this experiment, we first measured the pressure dependence of the absorption of the 193-nm laser radiation due to B_2H_6 and to BH_3CO in the optically thin region (<10% UV absorption). Our measured ratio of UV absorption coefficients for BH_3CO:B_2H_6 is 30:1, which is similar to that reported in the literature.[19] We then measured the infrared absorption due to BH_3 from both precursors under these conditions. Because the BH_3CO precursor results in much greater nascent BH_3 internal excitation, the experiments were performed with 1 Torr of N_2 buffer gas to thermalize the BH_3. The BH_3CO was purified and taken directly from the condensed sample to minimize decomposition. Since the quantum yield of BH_3 from B_2H_6 has been measured to be 2.0 ± 0.25 by Irion and Kompa,[20] we determined the quantum yield of BH_3 from BH_3CO by comparison to be greater than $0.7^{+0.3}_{-0.2}$. We report this measurement as a lower limit to the quantum yield because of the difficulty of vibrationally relaxing the ν_2 mode of BH_3 ($v'' > 0$) to BH_3 ($v'' = 0$) on a time scale prior to reaction or diffusion.

Discussion

The quantum yield measurement, $\Phi_{193}(BH_3) > 0.7^{+0.3}_{-0.2}$, provides a strong basis for assuming that simple B–C bond fission is the primary (and possibly the only) photochemical event following 193-nm excitation of BH_3CO:

$$BH_3CO \rightarrow BH_3 + CO \qquad (2)$$

From this result, we will now assume that reaction (2) is the *only primary photochemical process* occurring upon excitation at 193 nm. Since we observe BH_3 with a quantum yield of >0.7, it must be formed with less energy than required to dissociate to BH + H_2. This dissociation has been investigated both experimentally and theoretically by Caldwell et al.[21] They found a small activation barrier (ca. 2.5 kcal/mol) both by measuring the reverse reaction BH + $H_2 \rightarrow BH_3$ and from MCSCF-CI calculations on the BH_3 surface. It can be shown by an RRKM calculation that BH_3 excited 0.1 kcal/mol above the barrier has a lifetime of <1 ns.[22] Therefore, the most internal energy that BH_3 can contain is ~82 kcal/mol.

Irradiation of BH_3CO at 193 nm (51 813 cm^{-1}) might be expected to promote the lowest valence shell excitation in the molecule. BH_3CO exhibits a broad spectrum in the far ultraviolet with the lowest energy maxima at 55 800 (ϵ = 2400) and 63 800 cm^{-1} (ϵ = 11 500).[18] From ab initio calculations,[18,23] these transitions correspond to symmetry-allowed processes: $2e\sigma$(B–H) → $8a_1\sigma^*$(B–C) and $2e\sigma$(B–H) → $3e\pi^*$(C–O), respectively. As to the fate of the photoactivated BH_3CO, a simple argument would predict an instantaneous dissociation from the lowest excited state, since a σ^* state of the B–C bond is populated. Such an excitation would be predicted to yield a large amount of kinetic energy in the fragments and a relatively small amount of internal excitation in the CO photofragment. The nascent BH_3 fragment, however, would contain significant internal energy due to the reorganization of the molecular geometry from pyramidal to planar.

We can test this hypothesis by trying to understand our data in light of an impulsive model, which has been shown to be applicable to the case of direct dissociation.[24] It assumes that the BH_3CO is excited from the ground state to a single electronically excited state. It also assumes that the immediate effect of the photolysis is localized on the breaking bond so that the molecule can be considered to be quasidiatomic. For BH_3CO, the adiabatic excitation effectively converts the B–C (weak) σ bond to a strongly antibonding σ^* level. The BH_3 and CO halves of the molecule should be strongly repulsive. This repulsive potential should subsequently be converted to translational and internal energy of the BH_3 and CO fragments. In this model, the fraction of the available energy that is converted to translational energy of the fragments is determined from the ratio of the reduced mass of the B and C atoms to the reduced mass of BH_3 and CO fragments. The model predicts that 61% of the available energy will go into translation, which would result in 24.4 kcal/mol in CO kinetic energy compared to the ≥5 kcal/mol observed experimentally. This comparison suggests that the dissociation is not occurring directly from the initially excited electronic state.

A second approach to the question of direct dissociation is the Franck–Condon/golden rule model for calculating product vibrational energy distributions in fragmentation reactions, as proposed by Berry.[25,26] To calculate energy disposal into the

(18) Kanamori, H.; Hirota, E. *J. Chem. Phys.* **1987**, *86*, 3903.
(19) Robin, M. B. *Higher Excited States of Polyatomic Molecules*; Academic Press: New York, 1974; Vol. 1, pp 192–199.
(20) Irion, M. P.; Kompa, K. L. *J. Photochem.* **1986**, *32*, 139.
(21) Caldwell, N. J.; Rice, J. K.; Nelson, H. H.; Adams, G. F.; Page, M. *J. Chem. Phys.*, in press.
(22) Robinson, P. J.; Holbrook, K. A. *Unimolecular Reactions*; Wiley-Interscience: New York, 1972; Chapter 5.
(23) Snyder, L. C.; Basch, H. *Molecular Wave Functions and Properties: Tabulated from SCF Calculations in a Gaussian Basis*; Wiley: New York, 1972; T-154.
(24) Holdy, K. E; Klotz, L. C.; Wilson, K. R. *J. Chem. Phys.* **1970**, *52*, 4588.
(25) Berry, M. J. *Chem. Phys. Lett.* **1974**, *27*, 73.

diatomic fragment, the golden rule type expression for calculating the probability of forming CO in a given vibrational state, $P(f)$ is

$$P(f) \approx (2\pi/h)|\langle f|i\rangle|^2\rho(\epsilon) \quad (3)$$

where $|f\rangle\}$ and $|i\rangle$ are the complete set of product states and the initial state, respectively, and $\rho(\epsilon)$ is the density of states of the products. The product states in this case are the vibrational states of CO, and the initial state is taken to be the "dressed" CO oscillator of BH_3CO. By using Morse oscillator functions for $\{|f\rangle\}$ and $|i\rangle$, this model predicts a very small amount of vibrational excitation in the CO product $[(v'' = 1)/(v'' = 0) \approx 8 \times 10^{-4}]$. This calculated ratio, which is much smaller than the experimental value $[(v'' = 1)/(v'' = 0) = 0.33]$, results because there is very little difference in the CO bond length between the BH_3CO precursor[10] and the CO product. Berry's model should provide agreement in the limiting case of a direct dissociation. Our lack of agreement is consistent with our previous contention that BH_3CO does not dissociate directly from a single excited state.

Another possibility is that the photoactivated BH_3CO could undergo internal conversion to the ground electronic state prior to dissociation. Molecules with large rovibrational state densities can undergo rapid radiationless transitions to lower lying states or to the ground electronic state prior to dissociation.[27] BH_3CO has a high rovibrational state density resulting from the low-frequency symmetric bending mode (ν_8 = 313 cm^{-1}) and low-frequency stretch (ν_4 = 607 cm^{-1}) of the weak B–C bond.[14] From the ground state, one could imagine two limiting cases for dissociation: (1) a linear dissociation, in which the B–CO bond is stretched along the axis until it breaks into fragments; or (2) a bent dissociation, in which the CO twists off from the BH_3 fragment. Based on the previous results of a cold rotational distribution and our results here of a relatively "hot" (2760 K) vibrational distribution, we favor the linear transition state as the model for dissociation.

The total exoergicity of the photodissociation reaction 2 at 193 nm is ca. 127 kcal/mol. Statistical phase space models have been shown to predict nascent product vibrational energy distributions following photodissociation of polyatomic molecules in which there is no barrier to photodissociation in excess of the endoergicity.[28] If we assume the photolysis populates the internal states of the fragments according to statistical considerations alone, we can determine a prior distribution from phase space theory. We use the Whitten–Rabinovitch semiclassical treatment of vibrational–rotational systems to determine the density of states.[22] From the density of states, we can determine the probability distribution for the CO vibrational levels since the prior expectation is to populate every energetically allowed group of product states with a probability proportional to the number of states in the group.[29] If we assume that all the excess energy (see Figure 1) is available for statistical partitioning, we find that this approach predicts a greater degree of vibrational excitation in CO than was observed in the experiments. The predicted CO vibrational energy distribution can be fit to our data if we assume the energy available for statistical partitioning to be 35 kcal/mol. This smaller value for the available energy could be rationalized either by a large amount of energy in BH_3 electronic excitation or by an activation barrier in the dissociation which might preferentially channel some of the energy into translational energy. Production of electronically excited BH_3 seems very unlikely, since if the calculations of Swope et al.[16] are accurate, then we do not have enough energy to populate the electronically excited BH_3. Therefore, we conclude that the BH_3 is formed in its ground electronic state.

Another explanation for the low value obtained for the fit in the model could be the presence of an activation barrier in the dissociation channel. The relatively slow reaction[5] of BH_3 + CO supports this hypothesis. But, the low thermal stability of BH_3CO argues that, if a barrier exists, it must be far less than 90 kcal/mol. Bauer recommends a barrier of 23–25 kcal/mol for the thermal decomposition of BH_3CO.[10] An activation barrier to the dissociation might preferentially channel some of the total exoergicity (the fixed energy in RRKM terms[22]) of the reaction into translational energy in the fragments. This has been shown to be the case in the photodissociation of H_2CO, where a large barrier over and above the endothermicity of the reaction exits.[30] To obtain a correlation between our data and this statistical model, the barrier would have to be almost 90 kcal/mol in excess of the reaction endothermicity. This would no doubt impart a much larger fraction of translational energy than we observe. We conclude that the statistical phase space model described here is not an accurate account of the photodissociation dynamics of BH_3CO.

In spite of our ability to measure the energy distribution to numerous degrees of freedom in the separating photofragments, we are still not able to account for all the energy. This implies that a fair amount of energy is channeled into degrees of freedom that we do not measure quantitatively. The most likely possibilities for this energy is either internal energy in BH_3 or the existence of a low-lying (but not fluorescing) electronic state of BH_3. The presence of such an amount of internal energy in BH_3 implies that a nonstatistical partitioning of energy is operative in the photodissociation of BH_3CO. This needs to be probed directly to be properly understood, but the complete spectroscopy of BH_3 remains to be worked out. The second possibility of another electronic state of BH_3 is also a possibility that we cannot rule out completely but does seems unlikely.

Summary

The photodissociation of BH_3CO into the products BH_3 and CO at 193 nm leaves 127 kcal/mol to be distributed into kinetic and internal energy of the products. Since BH_3 is formed with a large quantum yield, it must have <82 kcal/mol to prevent dissociation to BH and H_2. Our measured CO internal energy accounts for ca. 5.9 kcal/mol in vibration (this paper) and ca. 0.6 kcal/mol in rotation.[11] We measure 15 kcal/mol as a lower limit to the total translational energy imparted to the photofragments. The actual translational energy must be considerably larger (>39 kcal/mol) to account for all the energy in the dissociation.

In the experiments reported in this paper, we have probed the photodissociation of BH_3CO in considerable detail by a variety of techniques. This is an interesting system because of its relatively large size and because of the large amount of energy to be disposed into the products. Although much progress has been made toward understanding the details of the energy disposal, several areas requiring further study remain. These include a more detailed analysis of the infrared spectra of BH_3, so that the degree of internal energy in the BH_3 photofragment can be measured experimentally. In addition, more accurate measurements of the translational energy of the fragments is necessary, perhaps by a time-of-flight technique. A better theoretical description of the photodissociation will also be required for a detailed understanding of the process.

Acknowledgment. We thank Luis Muñoz for his help with the computer graphics and the figure presentations.

Registry No. BH_3CO, 13205-44-2; BH_3, 13283-31-3; CO, 630-08-0.

(26) Berry, M. J. *Chem. Phys. Lett.* **1974**, *29*, 323, 329.
(27) Jortner, J.; Rice, S. A.; Hochstrasser, R. M. *Adv. Photochem.* **1969**, *7*, 149.
(28) Wittig, C.; Nadler, I.; Reisler, H.; Noble, M.; Cantanzarite, J. *J. Chem. Phys.* **1985**, *83*, 5581.
(29) Levine, R. D.; Bernstein, R. B. *Molecular Reaction Dynamics and Chemical Reactivity*; Oxford University Press: New York. 1987; p 274.
(30) Moore, C. B.; Weisshaar, J. C. *Annu. Rev. Phys. Chem.* **1983**, *34*, 525.